Nanotechnology **20** (2009) 175204 (5pp) doi:10.1088/0957-4484/20/17/175204

The dependence of the Schottky barrier height on carbon nanotube diameter for Pd–carbon nanotube contacts

Johannes Svensson[1], Abdelrahim A Sourab[1], Yury Tarakanov[2], Dong Su Lee[3], Seung Joo Park[4,5], Seung Jae Baek[4,5], Yung Woo Park[4,5] and Eleanor E B Campbell[1,6]

[1] Department of Physics, Göteborg University, SE-41296 Göteborg, Sweden
[2] Department of Applied Physics, Chalmers University of Technology, SE-41296 Gothenburg, Sweden
[3] Max-Planck-Institut für Festkörperforschung, Heisenbergstrasse 1, D-70569 Stuttgart, Germany
[4] School of Physics, Seoul National University, Seoul 151-747, Korea
[5] Nano Systems Institute–National Core Research Center, Seoul National University, Seoul 151-747, Korea
[6] School of Chemistry, Edinburgh University, West Mains Road, Edinburgh EH9 3JJ, UK

E-mail: ywpark@phya.snu.ac.kr and eleanor.campbell@ed.ac.uk

Received 4 December 2008, in final form 3 March 2009
Published 3 April 2009
Online at stacks.iop.org/Nano/20/175204

Abstract
Direct measurements are presented of the Schottky barrier (SB) heights of carbon nanotube devices contacted with Pd electrodes. The SB barrier heights were determined from the activation energy of the temperature-dependent thermionic emission current in the off-state of the devices. The barrier heights generally decrease with increasing diameter of the nanotubes and they are in agreement with the values expected when assuming little or no influence of Fermi level pinning.

(Some figures in this article are in colour only in the electronic version)

1. Introduction

It has been shown that carbon nanotube field effect transistors (CNTFETs) can act as Schottky barrier (SB) devices where the current is controlled by electrostatically modulating the thickness of a SB formed at the carbon nanotube (CNT)–metal contact if the channel is sufficiently short [1]. In order to achieve a high on-current and a low off-current, desirable for the integration of CNTFETs into electrical circuits, the SB height for holes (electrons) in the case of a p-type (n-type) device should be minimized. According to the Schottky–Mott theory, the SB height for electrons at the interface between a metal and a semiconductor is determined by the difference in work function of the metal and the electron affinity of the semiconductor [2]. However, for many conventional bulk semiconductor–metal contacts the SB height has a much weaker dependence on the metal work function than is expected from the Schottky–Mott theory, an effect known as Fermi level pinning. Several different theories have been developed that try to explain the pinning phenomenon. Some theories include the formation of states in the band gap of the semiconductor close to the contact that may arise due to defects or disorder or be induced by the metal, giving rise to an interface dipole altering the barrier height, while the chemical bond polarization theory attributes dipole formation to the polarization of bonds at the interface [3]. It has been theoretically predicted that the density of metal-induced gap states has to be very large in CNTs in order to induce any pinning of the Fermi level in a metal–CNT contact [4]. For end-bonded CNTs it has also been predicted that even for strong pinning the lack of effective screening will result in a barrier height which is determined only by the metal work function and the CNT band gap [5], which enables control of the barrier height by an appropriate choice of contact metal. It has been shown that metals with a high work function, such as Pd ($\phi = 5.12$ eV), give p-type behaviour with a high

on-current for CNTs with sufficiently large diameters [6, 7], indicating that the Fermi level of the metal is close to the valence band of the CNTs. Ti, which has a lower work function ($\phi = 4.4$ eV) than Pd, can give ambipolar characteristics with significant current for both holes and electrons, indicating that the Fermi level of the metal is close to the middle of the band gap of the CNT [8] while Ca with $\phi = 2.9$ eV gives n-type characteristics [9].

Even though many different metals have been studied as contacts for CNTFETs, the SB height has only been measured on single devices with Cr [10] and Ti [11] contacts which both give a similar barrier height for electrons and holes. Room temperature measurements of CNTFETs contacted with Pd, Ti or Al have shown that the on-current increases with increasing CNT diameter and metal work function, consistent with the behaviour expected from the ideal Schottky–Mott theory, but no SB heights were determined in these experiments [7, 12]. A measurement of the on-current cannot be directly correlated to the SB height since the exact metal–CNT bonding geometry has to be taken into account, e.g. a metal with poor coupling to CNTs should give a lower on-current than one which has a strong coupling, even although the SB heights are comparable [13, 14]. The effective SB height has been measured at gate voltages where there is significant band bending in the CNT [1, 15]. However, the effective SB does not give a good measure of the real barrier height since tunnelling dominates the transport at these gate voltages. Photocurrent [16] and scanning gate microscopy [17] experiments have also been used to image the SB between a metal and a CNT to study, for example, the depletion layer width, but quantitative results for the barrier heights were not extracted.

Here we present direct measurements of the SB heights for nine CNT devices contacted with Pd electrodes. The barrier heights, determined by studying the temperature dependence of the thermionic emission current, known as the activation energy method [18], are also directly correlated to the diameters of the CNTs. The SBs decrease with increasing diameter of the CNTs, and are in agreement with the ideal values estimated from the difference in work function, with the single exception of a large diameter CNT which we consider to be a small bundle of CNTs.

2. Fabrication

CNTs were grown on heavily n-doped Si wafers, with 400 nm thermally grown oxide, using thermal chemical vapour deposition (CVD). Catalyst islands with 5 nm Al_2O_3/1 nm Fe were patterned using electron beam lithography (EBL). The growth was performed for 15 min at 900 °C in a tube furnace with 500 sccm of CH_4 and 100 sccm of H_2. The grown CNTs were mostly single-walled as seen in a transmission electron microscope with an average diameter of 1.6 nm as measured using an atomic force microscope (AFM). Isolated CNTs were located using a scanning electron microscope and electrodes of 0.5 nm Ti/30 nm Pd with separations of 0.5–9 μm were patterned using EBL. The thin layer of Ti acts as an adhesion layer for Pd but does not significantly influence the contact properties since it is much thinner than the diameter of the CNTs [16]. If a significant amount of Ti were still to contact the CNTs the resulting SB height would be inhomogeneous and the current would be dominated by the lower Pd–CNT barrier [7].

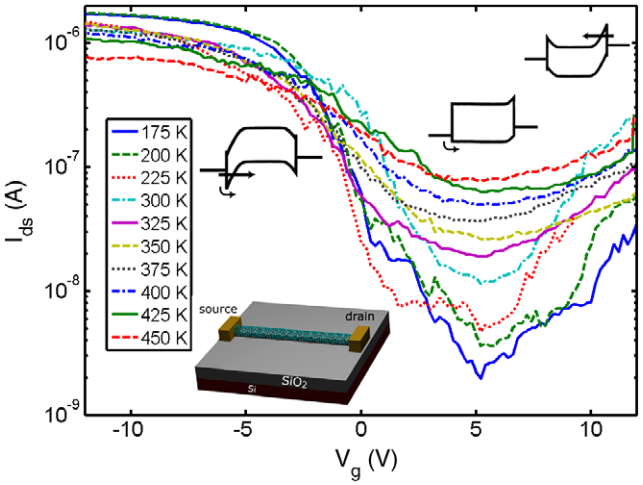

Figure 1. Transfer characteristics of a CNTFET at 10 different temperatures with $V_d = 100$ mV (the source electrode is grounded) and the schematic layout of a device. The curves have been laterally shifted to have the same threshold voltage (V_{th}) for all temperatures. Schematic band diagrams show hole transport dominated by tunnelling for low or negative V_g, thermionic emission of holes for intermediate V_g and electron transport via tunnelling at high V_g.

3. Electrical characterization and extraction of the SB height

The devices were electrically characterized in a vacuum (10^{-6} mbar) at temperatures down to 100 K using a source–drain bias of $V_d = 100$ mV (the source was grounded) and the Si substrate as a back gate. The transfer characteristics for a typical device at different temperatures are presented in figure 1. The minimum resistance of the devices in the on-state is around 70 kΩ and increases with increasing temperature, indicating that scattering within the CNTs is the main contribution to the resistance [19]. In contrast, the resistance in the off-state decreases with increasing temperature, indicating that thermally activated transport at the contacts is the main contribution to the resistance. All devices show ambipolar characteristics but with an order of magnitude larger on-current for negative gate voltages (V_g), which indicates that the barrier for holes is smaller than that for electrons. For negative V_g the bands will move up, making the SBs thinner and allowing for tunnelling of holes. The application of a high positive V_g will move the bands down, eventually making the SB for electrons thin enough to obtain a tunnelling current. For intermediate V_g at low V_d the band bending is very small, i.e. the SBs are too thick to allow tunnelling. In this regime the only possible transport mechanism is thermionic emission over the barriers, resulting in a current of

$$I_{ds} = A_s A_e^* T \exp(-q(\Phi_{SBe} - \Delta\Phi_{SBe})/k_B T) + A_d A_h^* T \exp(-q(\Phi_{SBh} - \Delta\Phi_{SBh})/k_B T) \quad (1)$$

where A_s (A_d) is the source (drain) contact area, A_e^* (A_h^*) is the effective Richardson's constant for electrons (holes), T is the temperature, k_B is the Boltzmann constant, Φ_{SBe} (Φ_{SBh}) is the electron (hole) SB height and $\Delta\Phi_{SBe}$ ($\Delta\Phi_{SBh}$) is the electron (hole) image force barrier lowering [20]. The exponent of T in the pre-exponential factors is set to 1 since the transport occurs in a 1D system [21].

The SB height is extracted by plotting the data from figure 1 in an Arrhenius plot (see figure 2(A)) which shows a linear relation between $\log(I_d/T)$ and $1/T$ for T = 300–450 K. An activation energy E_a is calculated from the slope of a linear fit to the Arrhenius plot and plotted as a function of V_g (see figure 2(B)). The linear fit is good close to the V_g corresponding to the maximum E_a which, together with the dominating p-type branch in figure 1, shows that only holes give a significant contribution to the current, enabling us to ignore the thermionic emission contribution from electrons in equation (1). The slope of the Arrhenius plot is smaller for the three lowest temperatures (T = 175–225 K), indicating that tunnelling, which has a weaker temperature dependence compared to thermionic emission, contributes significantly to transport at low temperatures [11]. E_a is also extracted from a temperature-dependent measurement of I_{ds} as a function of V_d, at a V_g corresponding to the minimum current (see figures 3(A)). Image force lowering of the barrier would give an E_a value proportional to the square root of the electric field. Thus a linear fit extrapolated to $V_d = 0$ V should give the actual barrier height. However, considerable image force lowering would only occur if there was a large band bending at the contact, i.e. at high V_d or high positive or negative V_g. In contrast, figure 3(C) shows that E_a is nearly constant for $V_d < 0.3$ V and decreases for larger V_d. This indicates that image force lowering and tunnelling are negligible at V_d = 100 meV and the bands are nearly flat. However, at high V_d, a combination of tunnelling and image force barrier lowering results in a smaller extracted E_a (see band diagrams in figure 3(C)). At other gate voltages E_a starts to decrease for smaller V_d, indicating that tunnelling has a larger impact on the transport at these V_g (see figure 3(C)). For the voltages used in our experiments, the arguments above can be used to simplify equation (1) as

$$I_{ds} = A_d A_h^* T \exp(-q\Phi_{SBh}/k_B T), \qquad (2)$$

which describes the current at small V_d and at a V_g corresponding to the flat band condition. Equation (2) is valid in a limited V_g range around the maximum of the E_a versus V_g plot, which corresponds to the SB height.

According to Appenzeller *et al* [11] a correct barrier height should be extracted at the starting point of the linear region in the E_a versus V_g curve since this corresponds to the thermionic emission limit. However, electron tunnelling currents from the source contact are disregarded in this assumption. As V_g is increased the bands move down, which increases the barrier for thermionic emission of holes but at the same time the electron barrier becomes thinner at the source allowing for tunnelling which lowers the activation energy. Others have found an activation energy which is nearly constant over a large V_g range and similar for holes and electrons and concluded that the Fermi level of their Cr contacts is positioned in the middle of the band gap of the CNT [10]. However, for similar barrier heights for holes and electrons an Arrhenius plot would not give a straight line. Therefore a fit corresponding to equation (1) using a sum of two exponentials has to be made to the measured data to accurately extract the barrier height [22].

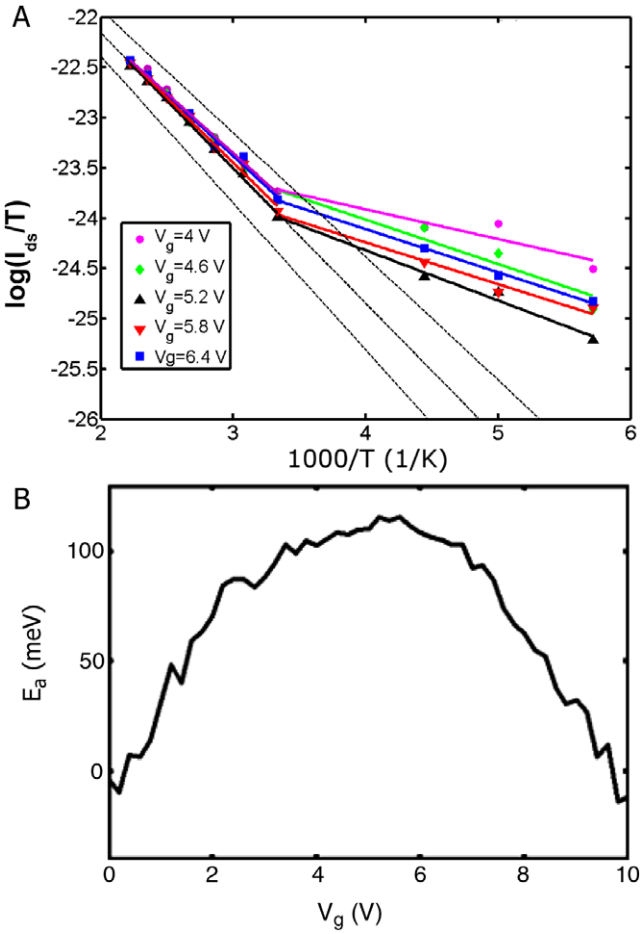

Figure 2. (A) Arrhenius plot with linear fits for five different gate voltages calculated from the transfer characteristics in figure 1. For $V_g = 5.2$ V the linear fit is good for the seven highest temperatures, indicating that thermionic emission dominates transport. The dashed lines show the theoretical result for thermionic emission over a barrier with a height of 106, 116 and 126 meV. (B) Activation energy as a function of V_g calculated from the linear fits for T = 300–450 K in (A). The maximum of 116 meV gives an estimate of the SB height. At high and low V_g the activation energy is reduced due to tunnelling.

The slope of the Arrhenius plots in figure 2(A) is lowered if we move away from the V_g corresponding to the maximum E_a. The two possible cases for the position of the bands at the maximum E_a are shown in figure 4. If the maximum E_a corresponds to the situation when bands are bent down with respect to the flat band condition ((2) in figure 4), decreasing V_g would result in a larger thermionic emission current and less tunnelling and thus the linear fit to the Arrhenius plot would be shifted up (as shown by the dashed lines in figure 2(A)). However, if the maximum E_a corresponds to the flat band situation ((5) in figure 4), decreasing V_g would give the same

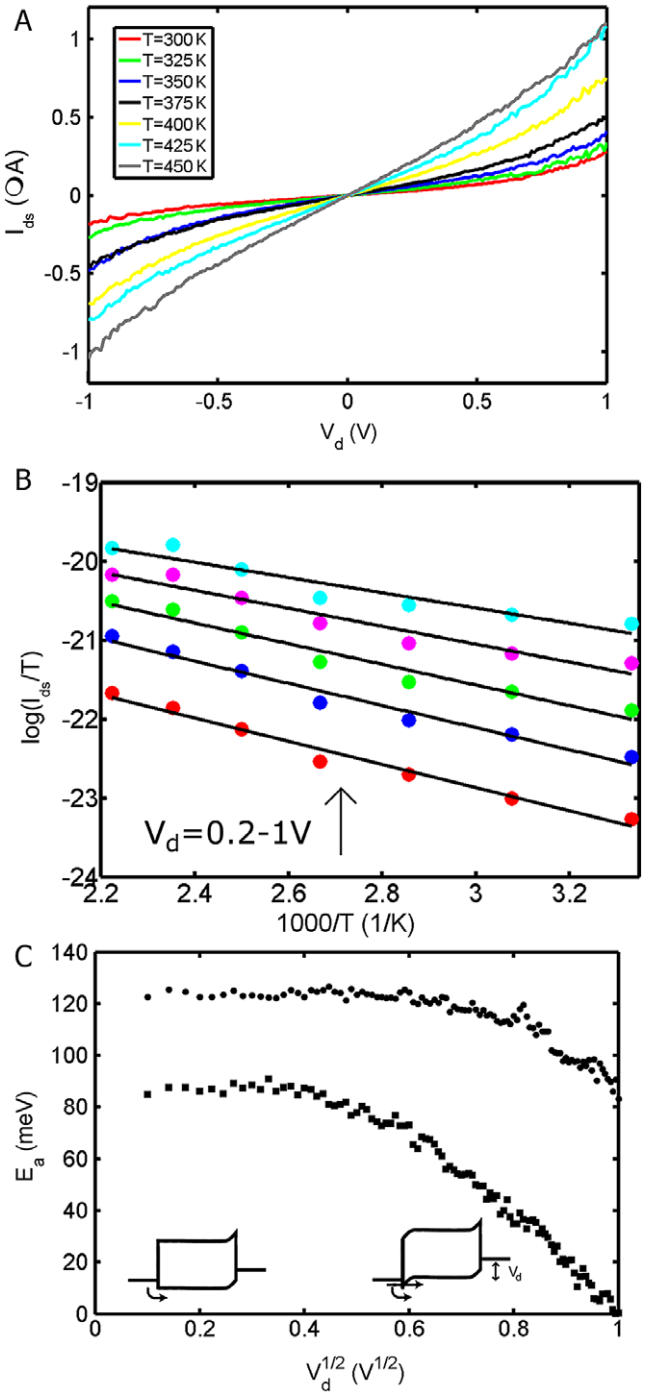

Figure 3. (A) I_{ds}–V_d curves for $T = 300$–450 K. (B) Arrhenius plots for $V_d = 0.2$–1 V (0.2 V step). (C) Activation energy as a function of square root of V_d at the V_g which gives minimum current (circles) and at $\Delta V_g = -2$ V (squares) from this gate voltage. The insets show schematic band diagrams at two different V_d.

thermionic emission current but a larger tunnelling current. Since the measured Arrhenius plots are not shifted laterally and the effective Richardson's constant or the contact area should not change during the measurement we conclude that the change in slope is due to increased tunnelling as we move away from the maximum E_a and thus the maximum is a good estimate of the real SB height. That the maximum E_a does

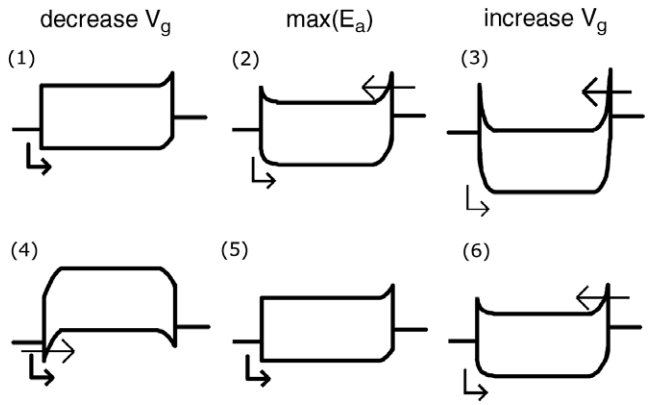

Figure 4. Schematic band diagrams for the two possible cases at maximum E_a. If the maximum E_a corresponds to the band situation in (2), decreasing V_g would result in an increased thermionic emission current and a decreased electron tunnelling current as shown in (1). If the maximum E_a corresponds to the band situation in (5), decreasing V_g would not affect the thermionic emission current but increase the hole tunnelling current. Increasing V_g would increase the tunnelling current for both cases.

not occur at $V_g = V_d = 100$ mV for which we expect to have flat band conditions at the drain side is most likely due to charge trapping in the oxide [23] or water molecules absorbed at the surface [24] which will shift the threshold voltage and give hysteresis in the transfer characteristics. We find that the measured activation energy is the same for interchanging the source and drain contact, i.e. the exact microscopic structure of the contact does not influence the SB height. Also repeated heating and cooling cycles, with exposure to air in between measurements, do not influence the measured SB height.

In the absence of Fermi level pinning in the CNT–metal contact the SB height for holes can be expressed as

$$\Phi_{SB} = \phi_{CNT} - \phi_M + E_g/2 \qquad (3)$$

where the band gap $E_g = 2a_{C-C}\gamma_0/d$ with $a_{C-C} = 1.42$ Å, $\gamma_0 = 2.89$ eV and d the CNT diameter [25]. The extracted SB heights for nine Pd contacted CNTs are plotted as a function of their diameter in figure 5. The diameters were determined by taking the average of at least 10 height measurements across different regions of each nanotube using an AFM. Included in the figure is also a theoretical estimate of the SB using (3) with $\phi_{CNT} = 4.9 \pm 0.1$ eV [26–28] and $\phi_{Pd} = 5.12$ eV [29]. It is clear that the SB height is lowered with increasing CNT diameter. The SB heights extracted from the measurements are typically higher than the theoretical estimate but are within the error limits, based on the ± 0.1 eV uncertainty in the CNT work function determination [26–28]. The device with the largest diameter nanotube in the series (2.9 nm) shows a clear deviation from the general trend with a SB significantly higher than the theoretical estimate (the data point is shown as an open square in figure 5). It is possible that a device with such a large diameter is a small bundle consisting of several CNTs that have been entangled during growth. A small bundle is difficult to distinguish from a single CNT using AFM. The extracted barrier height in such a device would be dominated by the CNT with the largest diameter but the AFM measurement would considerably overestimate the diameter.

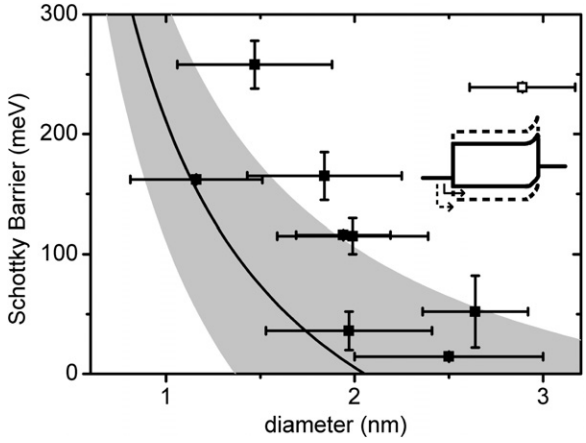

Figure 5. SB height as a function of CNT diameter for nine devices. The horizontal error bars are the standard deviation of multiple height profiles along a CNT obtained using an AFM. The vertical error bars are extracted from the uncertainty of the linear fits to the Arrhenius plots. The solid line shows a theoretical estimate of the SB for holes, assuming that the height is controlled by the difference in work function between Pd and CNT, and the shaded area shows the estimated SB for $\phi_{\mathrm{CNT}} = 4.8$–$5.0$ eV. The inset shows schematic band diagrams for a large (solid line) and a small (dashed line) diameter CNT.

4. Conclusions

We have shown that care has to be taken when extracting the SB height from activation energy measurements since there is a possibility that both electron and hole currents in CNTs depend on the band bending situation. We have found that the SB heights for CNTs contacted by Pd electrodes are inversely proportional to their diameter and are in agreement with values expected for a contact with little or no Fermi level pinning [4]. The absolute values determined are within the uncertainty given predominantly by the uncertainty in our knowledge of the CNT work function. We have taken the most accurate values in the literature determined by photoelectron spectroscopy and field emission microscopy, which give a value independent of nanotube diameter with an error of ± 0.1 eV [26–28]. To further study the influence of interface states and the effect of Fermi level pinning in CNT–metal contacts, the SB height for metals with different work functions should be studied. However, due to the large uncertainty in the diameter and the work function of the CNTs, work on devices with multiple contacts of different metals on the same CNT is in progress.

Acknowledgments

The authors thank Johan Piscator and Oleg Nerushev for fruitful discussions. Financial support from Vetenskapsrådet, the K and A Wallenberg Foundation, STINT and the Korea Foundation for International Cooperation of Science and Technology (KICOS) through a grant provided by the Korea Ministry of Education, Science and Technology (MEST) (GPP K20602000006-07E0200-00610) is gratefully acknowledged. YT and EEBC acknowledge the support of the European Commission through the FP6 grant NanoRF. This publication reflects the views of the authors and not necessarily those of the EC. The EC is not liable for any use that may be made of the information contained herein.

References

[1] Appenzeller J, Knoch J, Derycke V, Martel R, Wind S and Avouris Ph 2002 *Phys. Rev. Lett.* **89** 126801
[2] Schottky W 1940 *Phys. Z.* **41** 570
[3] Tung R T 2001 *Phys. Rev.* B **64** 205310
[4] Leonard F and Talin A A 2006 *Phys. Rev. Lett.* **97** 026804
[5] Leonard F and Tersoff J 2000 *Phys. Rev. Lett.* **84** 4693
[6] Javey A, Guo J, Wang Q, Lundstrom M and Dai H 2003 *Nature* **424** 654
[7] Chen Z, Appenzeller J, Knoch J, Lin Y M and Avouris Ph 2005 *Nano Lett.* **5** 1497
[8] Martel R, Derycke V, Lavoie C, Appenzeller J, Chan K K, Tersoff J and Avouris Ph 2001 *Phys. Rev. Lett.* **87** 256805
[9] Nosho Y, Ohno Y, Kishimoto S and Mizutani T 2006 *Nanotechnology* **17** 3412
[10] Chen Y F and Fuhrer M S 2006 *Nano Lett.* **6** 2158
[11] Appenzeller J, Radosavljevic M, Knoch J and Avouris Ph 2004 *Phys. Rev. Lett.* **92** 048301
[12] Kim W, Javey W, Tu E, Cao J, Wang W and Dai H 2005 *Appl. Phys. Lett.* **87** 173101
[13] Shan B and Cho K 2004 *Phys. Rev.* B **70** 233405
[14] Palacios J J, Tarakeshwar P and Kim D M 2008 *Phys. Rev.* B **77** 113403
[15] Inami N, Mohamed M A, Shikoh E and Fujiwara A 2008 *Appl. Phys. Lett.* **92** 243115
[16] Freitag M, Tsang J C, Bol A, Yuan D, Liu J and Avouris Ph 2007 *Nano Lett.* **7** 2037
[17] Marcus F, Radosavljevic R, Yangxin Z, Johnson A T and Walter F S 2001 *Appl. Phys. Lett.* **79** 3326
[18] Sze S M 1969 *Physics of Semiconductor Devices* (New York: Wiley–Interscience)
[19] Purewal M S, Hong B H, Ravi A, Chandra B, Hone J and Kim P 2007 *Phys. Rev. Lett.* **98** 186808
[20] Sze S M, Coleman D J and Loya A Jr 1971 *Solid-State Electron.* **14** 1209
[21] Rekhviashvili S S 2006 *Tech. Phys. Lett.* **32** 123
[22] Behnam A, Johnson J, Choi Y, Noriega L, Ertosun M G, Wu Z, Rinzler A G, Kapur P, Saraswat K C and Ural A 2008 *J. Appl. Phys.* **103** 114315
[23] Fuhrer M S, Kim B M, Dürkop T and Brintlinger T 2002 *Nano Lett.* **2** 755
[24] Kim W, Javey A, Vermesh O, Wang Q, Li Y and Dai H 2003 *Nano Lett.* **3** 193
[25] Joselevich E and Lieber C M 2002 *Nano Lett.* **2** 1137
[26] Suzuki S, Bower C, Watanabe Y and Zhou O 2000 *Appl. Phys. Lett.* **76** 4007
[27] Sun J P, Zhang Z X, Hou S M, Zhang G M, Gu Z N, Zhao X Y, Liu W M and Xue Z Q 2002 *Appl. Phys.* A **75** 479
[28] Shiraishi M and Ata M 2001 *Carbon* **39** 1913
[29] Michaelson H B 1977 *J. Appl. Phys.* **48** 4729